crystals

MDPI

Article

Crystal Structure of the 23S rRNA Fragment Specific to r-Protein L1 and Designed Model of the Ribosomal L1 Stalk from *Haloarcula marismortui*

Azat Gabdulkhakov *, Svetlana Tishchenko, Alisa Mikhaylina, Maria Garber, Natalia Nevskaya and Stanislav Nikonov

Institute of Protein Research, Russian Academy of Sciences, Institutskaya 4, 142290 Puschino, Moscow Region, Russian Federation; sveta@vega.protres.ru (S.T.); alisamikhaylina15@gmail.com (A.M.); garber@vega.protres.ru (M.G.); nevskaya@protres.ru (N.N.); nikonov@vega.protres.ru (S.N.)
* Correspondence: azat@vega.protres.ru; Tel.: +7-4967-318-475

Academic Editors: Helmut Cölfen and Albert Guskov
Received: 13 December 2016; Accepted: 29 January 2017; Published: 2 February 2017

Abstract: The crystal structure of the 92-nucleotide L1-specific fragment of 23S rRNA from *Haloarcula marismortui* (Hma) has been determined at 3.3 Å resolution. Similar to the corresponding bacterial rRNA fragments, this structure contains joined helix 76-77 topped by an approximately globular structure formed by the residual part of the L1 stalk rRNA. The position of HmaL1 relative to the rRNA was found by its docking to the rRNA fragment using the L1-rRNA complex from *Thermus thermophilus* as a guide model. In spite of the anomalous negative charge of the halophilic archaeal protein, the conformation of the HmaL1-rRNA interface appeared to be very close to that observed in all known L1-rRNA complexes. The designed structure of the L1 stalk was incorporated into the *H. marismortui* 50S ribosomal subunit. Comparison of relative positions of L1 stalks in 50S subunits from *H. marismortui* and *T. thermophilus* made it possible to reveal the site of inflection of rRNA during the ribosome function.

Keywords: *Haloarcula marismortui*; ribosomes; archaea; 23S rRNA; X-ray crystallography

1. Introduction

Haloarcula marismortui (Hma) is an extreme halophilic archaeon which is able to grow at salt concentrations close to saturation. The ribosome of this archaeon functions at 3.5–4.0 M salinity at up to 60 °C. Such conditions usually cause the dissociation of nucleoprotein assemblies and denaturation of isolated proteins. However, the ribosomal particles obtained from this organism retain their integrity and activity for long periods [1]. Moreover, the structure of the 50S ribosomal subunit from *H. marismortui* is the only crystal structure of an archaeal ribosomal particle that has been determined to date [2]. Unfortunately, the first model of the Hma 50S subunit and the last revised one [3] contain some gaps. In particular, the functionally important mobile L1 protuberance (stalk) is not completely visualized.

The L1 stalk includes protein L1 and helices 76, 77, 78 of 23S rRNA. It is a strongly conserved component of ribosomes in all domains of life. This stalk is involved in the exit of deacylated tRNA from the ribosome and is found in different relative positions in the structures of *T. thermophilus* 70S ribosome-tRNA complexes [4,5], the isolated *D. radiodurans* 50S subunit [6] and the eukaryotic ribosome [7]. The HmaL1 stalk was modeled and incorporated by docking into a low-resolution 9 Å map of the Hma 50S ribosomal subunit [8], but a clear electron density at the expected site of the L1 protein was absent. The trials to find an interpretable electron density for this ribosomal region in the 2.4 Å electron-density map at the revisiting *H. marismortui* large ribosomal subunit [3] led only to the visualization of nucleotides 2137–2149 and 2226–2237 of helix 76 of the 23S rRNA.

Similar to other *H. marismortui* proteins [9] the HmaL1 surface has a high number of acidic residues (24.5%) compared with basic ones (10.8%) (Figure S1a), and all experimental data on HmaL1 were obtained at high salt concentration specific for the proteins of the ribosome from *H. marismortui.* Despite the large negative charge, HmaL1 can specifically bind the 23S rRNA fragment from *Escherichia coli* [1]. This suggests that the structure of the RNA-binding site of HmaL1 is similar to that in other L1 proteins. All our attempts to obtain crystals of HmaL1 or its complexes with specific rRNA fragments failed, possibly owing to the anomalous negative charge of this protein. Therefore, having started from the known structures of L1 proteins from other organisms we built a model of HmaL1 and refined it by molecular dynamics methods (in press). This model was very close to the crystal structure of the L1 protein from *Methanocaldococcus jannashchii* (MjaL1) charged positively [10]. However, the crystal structures and mutual arrangement of HmaL1 and RNA moieties within the HmaL1 stalk remain unknown. The main aim of our work was to determine the structure of this important ribosomal domain to supplement the model of the Hma 50S ribosomal subunit.

Here, we report the 3.3 Å resolution structure of the rRNA moiety of the L1 stalk of the 50S ribosomal subunit from *H. marismortui.* Similar to 23S rRNA fragments from other organisms, this structure contains long helix 76-77 topped by an approximately globular structure formed by the residual part of the L1-specific 23S rRNA. The region of the surface responsible for the HmaL1 binding is very close to that in the *E.coli* and *T. thermophilus* ribosomes. Based on this finding, the structure of the whole stalk was obtained by docking HmaL1 to the fragment of 23S rRNA using the TthL1-rRNA complex as a guide model. The designed structure was incorporated into the *H. marismortui* 50S subunit. Determining the crystal structure of the L1-specific Hma rRNA fragment and designing the HmaL1 stalk model significantly supplemented the known structure of the 50S ribosomal subunit from *H. marismortui.* In addition, comparison of relative positions of L1 stalks in the 50S subunits from *H. marismortui* and *T. thermophilus* made it possible to reveal the rRNA inflection site, which permits the L1-stalk to move during ribosome function.

2. Results and Discussion

2.1. Structure of the L1-Specific rRNA Fragment from H. marismortui

It is generally accepted that the rRNA moiety of the *H. marismortui* L1 stalk consists of three helices (H76, H77, H78) and three loops (A, B, C) (Figure 1a). Nevertheless, the crystal structures of the isolated L1 stalk [11] and 70S ribosomes [5,12,13] from *T. thermophilus* show that helices 76 and 77 form one helical structure, while the helix 78 consists of two parts (H78a and H78b) that are approximately perpendicular to each other. The 92 nucleotide fragment of 23S rRNA from *H. marismortui* used in this work contains a part of long helix 76-77 topped by an approximately globular structure formed by the residual part of the L1 stalk rRNA (Figure 1b).

The long axis of inertia of this globular moiety is tilted approximately 25 degrees with respect to the H76-H77 axis and there is a wide hole with minimal diameter more than 7 Å in its center. The internal surface of the hole is generally formed by phosphate groups and is charged negatively. At concentration of NaCl close to saturation (typical conditions for the Dead Sea) this hole could be filled by sodium ions. Loops A and B together with the closing loop of H78b form a helix-like structure, which is stabilized by five triplets: U2152•A2191•G2188, A2155•A2160•G2213, G2156•A2216•U2212, A2158-U2217•G2211 and U2159•G2192-C2187. Figure 2 shows the electron density in the region of one of these triplets and in the region of loop C. Loop C ensures a sharp bend between H78a and H78b and forms a deep negatively charged cavity stabilized by two triplets: C2177-G2202•A2178 and G2179-C2201•C2198.

The asymmetric unit contains two RNA molecules related by the two-fold non-crystallographic axis parallel to joint helix 76-77. Both molecules have similar conformations with an r.m.s. deviation of 0.964 Å for all P atoms. The bases of U2205, G2204, A2171 and C2172 of symmetry-related molecules form an integrated stacking line stabilizing the crystal.

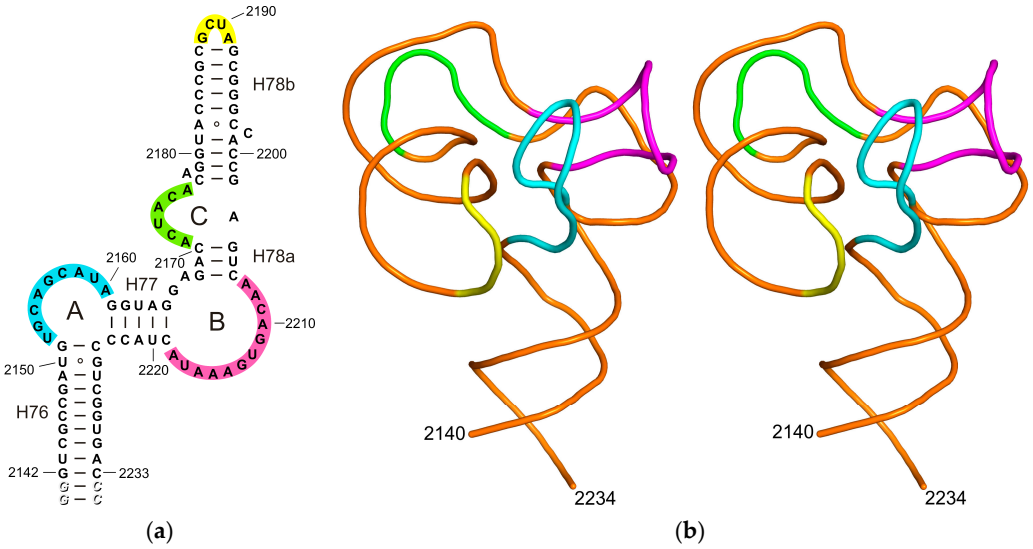

Figure 1. (**a**) Secondary structure of the 92-nt 23S rRNA fragment from *H. marismortui* elongated by two additional G-C base pairs shown in grey and italics; (**b**) Stereo view of the crystal structure of the rRNA fragment. On both panels, loop A is shown in cyan, B—in magenta, C—in green and the closing loop of H78b—in yellow.

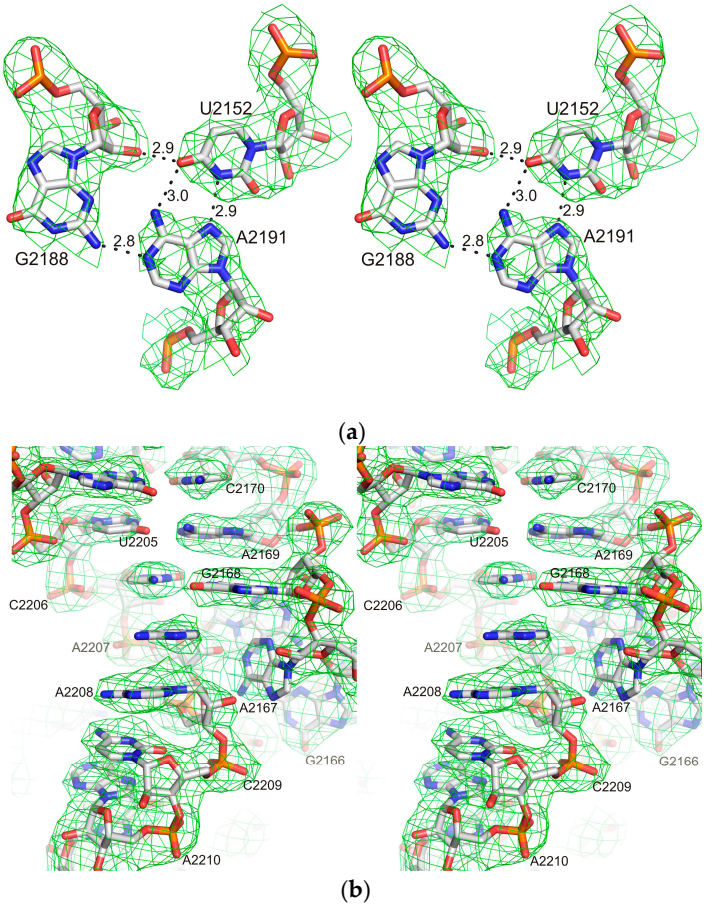

Figure 2. A stereoview showing the $2F_o$-F_c map at 3.3 Å resolution contoured at 1.0 σ in the region of (**a**) triplet U2152●A2191●G2188 and (**b**) loop C.

The L1-specific fragment of 23S rRNA from *H. marismortui* is structurally close to the corresponding region of 23S rRNA from *T. thermophilus*. The best matching is found for the top globular structures with an rmsd of 1.16 Å for 39 P atoms (Figure 3). The main differences are found in the loop C connecting helices 78a and 78b. The narrow deep groove formed by C2198-A2203 and A2174-A2176 in *H. marismortui* 23S rRNA is absent in *T. thermophilus* 23S rRNA.

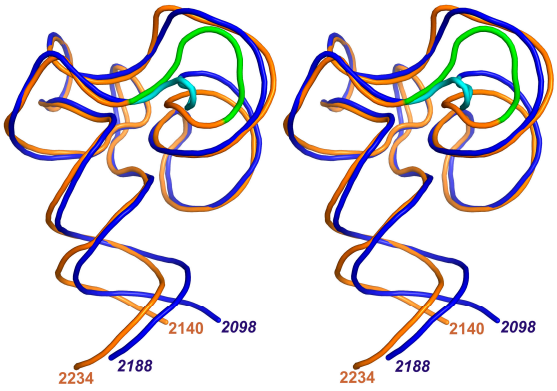

Figure 3. Superposition of the L1 stalk RNAs from *H. marismortui* (gold, loop C—green) and *T. thermophilus* (blue, loop C—cyan). Stereo view was constructed using least-squares minimization of differences in the P atom coordinates of the globular part of RNA.

2.2. The Designed Model of the HmaL1 Stalk

The RNA part of the HmaL1-rRNA interface is very close to that in the TthL1-rRNA one (rmsd = 0.801 Å for 18 P atoms). This also assumes a close similarity of the protein parts. On this basis, the structure for the L1 stalk was constructed by docking the designed HmaL1 model simulated by molecular dynamics methods at 200 ns trajectory (in press) to the determined fragment of 23S rRNA. The structure of the *T. thermophilus* L1-rRNA complex was used as a guide model. Initially the RNA part of the TthL1-rRNA interface was superimposed onto the corresponding region of the HmaRNA and then the HmaL1 β-sheet of domain I was superimposed onto that of TthL1 (rmsd = 0.552 Å for 25 Cα atoms). The complex was refined with *PHENIX* using the simple dynamics procedure [14]. The designed structure of the *H. marismortui* L1 stalk is shown in Figure 4.

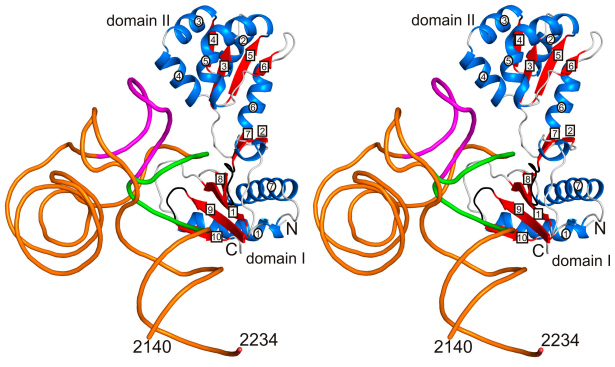

Figure 4. Stereo view of the designed L1 stalk from *H marismortui*. In HmaL1, α-helices (blue) and β-strands (red) are numbered. The RNA phosphate trace is shown in gold accepting helix 77 which is in green and loop B which is in magenta.

Similar to other L1-rRNA complexes [11,15] the protein L1 of the *H. marismortui* L1 stalk acts as tongs that enclose helix 77 of 23S rRNA (Figure 4). The tongs consist of a central part formed by β-sheet of domain I and two movable arms formed by loops β7-β8 and β9-β10. Loop α1-β1 protects

arm β9-β10 from the solvent. Five amino acid residues (Arg153, Arg157, Arg158, His161 and Arg165) located on the outer surface of the HmaL1 β-sheet of domain I (Figure S1b) form a positively charged cluster unique among L1 proteins. All residues of this cluster are involved in hydrogen bonds and salt bridges with the 23S rRNA fragment. Possibly this unique cluster induces an additional stability of the HmaL1-rRNA complex in high salt conditions. The surface formed by loop β1-β2 of HmaL1 and helix-like structure of 23S rRNA can serve as a site for tRNA. Domain II is located close to loop B of the 23S rRNA but there is no contact between them. The role of this domain bearing very high negative charge is still unknown in terms of the function of the *H. marismortui* ribosome.

2.3. Incorporation of the L1-Specific 23S rRNA Fragment into 50S Subunit of the H. marismortui Ribosome

Since the recent spatial model of the isolated *H. marismortui* 50S subunit contains part of helix 76 [3], we are able to incorporate the structure of L1-specific 23S rRNA fragment into this subunit. The regions 2140-2148 and 2228-2234 presented in both the determined RNA fragment and the 50S subunit were superimposed with an rmsd of 2.171 Å (Figure 5a). The L1 stalk has no direct interactions with the body of the 50S subunit although protein L1 is in close proximity to its helices 22 and 68. In HmaL1, helices α1 and α8, loops β1-β2 and α8-β9 directed to the 50S subunit body are able to come into contact with it during movements of the L1 stalk.

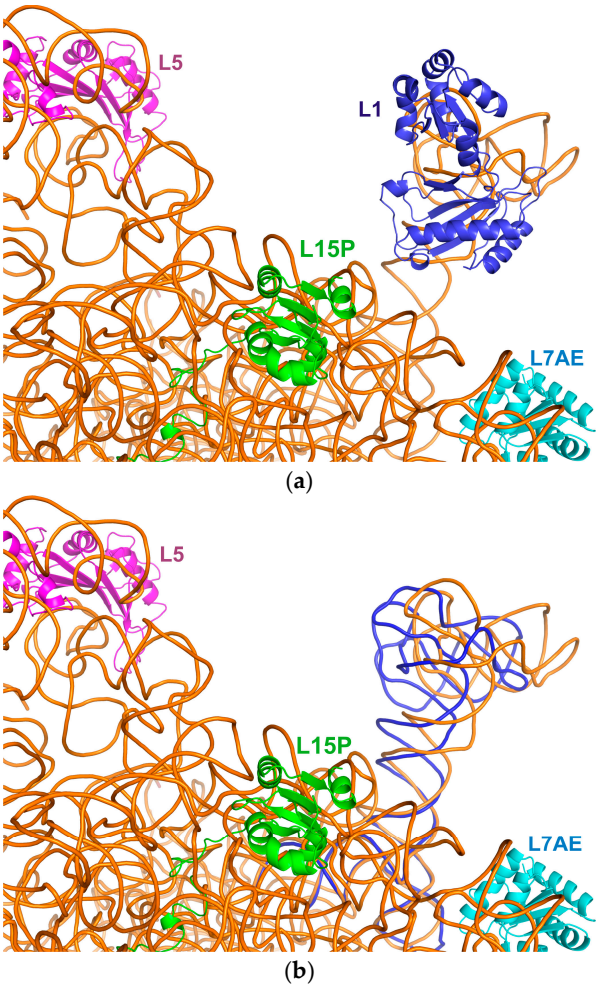

Figure 5. (**a**) Incorporation of the designed HmaL1 stalk into the model of the 50S subunit of *H. marismortui*; (**b**) Superposition of RNA from the TthL1 stalk (blue) onto Hma RNA with least-squares minimization of differences in P atom coordinates of the part of helix 76 deepened in the body of the 50S subunit.

Superposition of the *T. thermophilus* rRNA fragment onto the part of *H. marismortui* helix 76 tightly associated with the 50S subunit makes it possible to reveal the site of inflection of rRNA during function of the ribosome (Figure 4b). This bend is provided by the wobble pairs U2140•G2235 and G2141•U2234 in the *H. marismortui* helix 76 and the corresponding wobble pairs in the *T. thermophilus* one. Notice that these base pairs were also found in the *E.coli* ribosome [16]. Rotation around the axis, which approximately passes through the phosphorus atoms of nucleotides U2140 and G2235, induces displacement of the most remote points of the RNA globular parts up to 20 Å. Incorporation of both HmaL1 and TthL1 stalks into the 50S ribosomal subunit of *H. marismortui* shows that the top of the L1 stalk moves between proteins L7AE and L5.

3. Materials and Methods

3.1. RNA Fragment Preparation

The 23S rRNA fragment was obtained by transcription from a synthetic DNA template, using T7 RNA polymerase. The fragment included 92 nucleotides of 23S rRNA *H. marismortui* and additional two G-C pairs to form the restriction site for SmaI. RNA was purified by electrophoresis on denaturing (7 M urea) 10% (*w*/*v*) acrylamide (19:1, acrylamide/bis- acrylamide) gels, using 90 mM Tris-borate (pH 8.2), 1 mM EDTA as a running buffer. RNA was eluted by the 50 mM Tris-HCl buffer (pH 7.5, 25 °C), 1 mM EDTA, purified by an anion-exchange (DEAE-Toyopearl) chromatography, precipitated by ethanol and dissolved in water at concentration 3 mg/mL.

3.2. Crystallization

The RNA fragment was heated at 60° C for 10 min and incubated at 22° C for 30 min. Crystallization experiment was performed at room temperature using the hanging-drop vapor-diffusion method on siliconized glass cover slides in Linbro plates. Drops were made by mixing 1.4 µL RNA fragment with 2 µL well solution consisting of 20% *v*/*v* 2-methyl-2,4-pentanediol, 0.05 M MES, pH 5.6, 0.1 M magnesium acetate (condition No. 3 of Natrix from Hampton Research) and 0.4 µL 1M magnesium chloride. Crystals appeared in 2–3 days and grew to the maximum dimensions of 0.05 × 0.1 × 0.1 mm within one week. Prior to cooling in liquid nitrogen, the crystals were transferred into the 30% *v*/*v* 2-methyl-2.4-pentanediol, 0.05 M MES, pH 5.6.

3.3. Data Collection and Structure Determination

Diffraction data were collected to 3.3 Å resolution on the ID30A-3 beamline of the ESRF (Grenoble, France) equipped with Eiger X 4M fast detector (Dectris, Baden-Daettwil, Switzerland). An oscillation angle of 0.1° (according to the new standard protocol) and a crystal-to-detector distance of 614 mm were used. Data were processed and scaled with the *XDS* package [17]. The crystals of the HmaRNA belonged to space group $P4_12_12$ with unit cell parameters a = b = 136.84, c = 70.11 Å and two molecules in the asymmetric unit.

The structure was solved by molecular replacement with *Phaser* [18] using the structure of 80 nt fragment of 23S rRNA from *T. thermophilus* (PDB entry 3U4M; [11]) as a search model. Water molecules and metal ions were removed from the model. The initial model was subjected to crystallographic refinement with *REFMAC5* [19]. Manual rebuilding of the model was carried out in *Coot* [20]. The final model of the HmaRNA, refined to an R factor of 22.6% and R_{free} of 29.1% at 3.3 Å resolution, includes 190 nucleotides, 19 water molecules, eight magnesium ions, and calcium ion. Data and refinement statistics are summarized in Table 1. The coordinates and structure factors have been deposited in the Protein Data Bank (PDB entry 5ML7). Figures were prepared using PyMOL [21].

Table 1. Data collection and refinement statistics.

Data collection	
Wavelength (Å)	0.8266
Space group	$P4_12_12$ (No. 92)
Unit-cell parameters (Å, °)	a = b = 136.84, c = 70.11, α = β = γ = 90
Resolution limits (Å)	30.0–3.3 (3.5–3.3)
Completeness (%)	96.6 (93.0)
Measured reflections	53948 (7363)
Unique reflections	10134 (1551)
Rmerge (%)	15.0 (45.2)
Mean I/σ(I)	6.68 (3.2)
Redundancy	5.32 (4.74)
Refinement	
Resolution (Å)	30.0–3.30 (3.39–3.30)
No. of reflections	9 674 (665)
R factor (%)	22.6 (35.4)
Free R factor (%)	29.14 (50.6)
Average overall B factor ($Å^2$)	65.3
R.m.s. deviations	
Bond lengths (Å)	0.008
Bond angles (°)	1.72
PDB code	5ML7

Data were collected at 100K. Values in parentheses are for the last resolution shell.

4. Conclusions

Because of its overall negative charge, R-protein Hma L1 is significantly different from all L1 proteins which structures were determined. Although we could not crystallize this protein and its complex with the rRNA fragment, our results show that conformation of the L1-binding site of the Hma 23S rRNA is similar to that observed in other known structures of prokaryotic ribosomes. Together with the previous data on the HmaL1 structure obtained by modeling and MD simulation, the presented results enable us to build a reliable model of the HmaL1 stalk which confirms the close shape of this ribosomal element in all organisms regardless of the different overall charge of L1 proteins.

Supplementary Materials: The following are available online at www.mdpi.com//2073-4352/7/2/37/s1. Figure S1. (a) HmaL1 amino acid sequence. Negatively charged amino acids are indicated with a yellow background and positively charged with a green one. α-helices are shown as blue cylinders and β-strands as red arrows; (b) Stereo view of Cα trace of HmaL1 model. Cα atoms of charged amino acids are shown with circles (black for negative charge, grey for positive one). HmaL1 positively charged cluster unique among L1 proteins is indicated by side chains.

Acknowledgments: This work was supported by Russian Foundation for Basic Research (No. 14-04-00571, 14-04-00406) and the Program of RAS on Molecular and Cellular Biology.

Author Contributions: Svetlana Tishchenko and Alisa Mikhaylina performed the biochemical experiments (RNA fragment preparation and crystallization), Azat Gabdulkhakov performed X-ray experiments and solved crystal structure, Maria Garber designed the experiments, Natalia Nevskaya and Stanislav Nikonov analyzed results and wrote the paper.

Conflicts of Interest: The authors declare no competing financial interests.

References

1. Evers, U.; Franceschi, F.; Boddeker, N.; Yonath, A. Crystallography of halophilic ribosome: The isolation of an internal ribonucleoprotein complex. *Biol. Chem.* **1994**, *50*, 3–16. [CrossRef]
2. Ban, N.; Nissen, P.; Hansen, J.; Moore, P.B.; Steitz, T.A. The complete atomic structure of the large ribosomal subunit at 2.4 Å resolution. *Science* **2000**, *289*, 905–920. [CrossRef] [PubMed]
3. Gabdulkhakov, A.; Nikonov, S.; Garber, M. Revisiting the *Haloarcula marismortui* 50S ribosomal subunit model. *Acta Crystallogr. Sect. D Biol. Crystallogr.* **2013**, *69*, 997–1004. [CrossRef] [PubMed]

4. Yusupov, M.M.; Yusupova, G.Z.; Baucom, A.; Lieberman, K.; Earnest, T.N.; Cate, J.H.D.; Noller, H.F. Crystal structure of the ribosome at 5.5 Å resolution. *Science* **2001**, *292*, 883–896. [CrossRef] [PubMed]
5. Gao, Y.-G.; Selmer, M.; Dunham, C.M.; Weixlbaumer, A.; Kelley, A.C.; Ramakrishnan, V. The structure of the ribosome with elongation factor G trapped in the posttranslocation state. *Science* **2009**, *326*, 694–699. [CrossRef] [PubMed]
6. Harms, J.; Schluenzen, F.; Zarivach, R.; Bashan, A.; Gat, S.; Agmon, I.; Bartels, H.; Franceschi, F.; Yonath, A. High resolution structure of the large ribosomal subunit from mesophilic eubacterium. *Cell* **2001**, *107*, 679–688. [CrossRef]
7. Ben-Shem, A.; Jenner, L.; Yusupova, G.; Yusupov, M. Crystal structure of the eukaryotic ribosome. *Science* **2010**, *320*, 1203–1209. [CrossRef] [PubMed]
8. Klein, D.J.; Moore, P.B.; Stetz, T.A. The role of ribosomal proteins in the structure assembly, and evolution of the large ribosomal subunit. *J. Mol. Biol.* **2004**, *340*, 141–177. [CrossRef] [PubMed]
9. Córdova, D.I.C.; Ruíz, R.M.C.; Díaz, J.C.M.; López, J.A.C.; Rodríguez, J.A.G. *Haloarcula marismortui*, eighty-four years after its discovery in the Dead Sea. *Int. J. Eng. Res. Technol.* **2014**, *3*, 1257–1267.
10. Nevskaya, N.; Tishchenko, S.; Fedorov, R.; Al-Karadaghi, S.; Liljas, A.; Kraft, A.; Piendl, W.; Garber, M.; Nikonov, S. Archaeal ribosomal protein L1: The structure provides new insights into RNA binding of the L1 protein family. *Structure* **2000**, *8*, 363–371. [CrossRef]
11. Tishchenko, S.; Gabdulkhakov, A.; Nevskaya, N.; Sarskikh, A.; Kostareva, O.; Nikonova, E.; Sycheva, A.; Moshkovskii, S.; Garber, M.; Nikonov, S. High-resolution crystal structure of the isolated ribosomal. *Acta Crystallogr. Sect. D Biol. Crystallogr.* **2012**, *68*, 1051–1057. [CrossRef] [PubMed]
12. Feng, S.; Chen, Y.; Gao, Y.-G. Crystal structure of 70S ribosome with both cognate tRNAs in the E and P sites representing an authentic elongation complex. *PLoS ONE* **2013**, *8*, 1–10. [CrossRef] [PubMed]
13. Polikanov, Y.S.; Melnikov, S.V.; Söll, D.; Steitz, T.A. Structural insights into the role of rRNA modifications in protein synthesis and ribosome assembly. *Nat. Struct. Mol. Biol.* **2015**, *22*, 342–344. [CrossRef] [PubMed]
14. Afonine, P.V.; Grosse-Kunstleve, R.W.; Echols, N.; Headd, J.J.; Moriarty, N.W.; Mustyakimov, M.; Terwilliger, T.C.; Urzhumtsev, A.; Zwart, P.H.; Adams, P.D. Towards automated crystallographic structure refinement with phenix.refine. *Acta Crystallogr. Sect. D Biol. Crystallogr.* **2012**, *68*, 352–367. [CrossRef] [PubMed]
15. Nikulin, A.; Eliseikina, I.; Tischenko, S.; Nevskaya, N.; Davydova, N.; Platonova, O.; Piendl, W.; Selmer, M.; Liljas, A.; Drygin, D.; et al. Structure of the L1 protuberance in the ribosome. *Nat. Struct. Biol.* **2003**, *10*, 104–108. [CrossRef] [PubMed]
16. Schuwirth, B.S.; Borovinskaya, M.A.; Hau, C.W.; Zhang, W.; Vila-Sanjurjo, A.; Holton, J.M.; Cate, J.H.D. Structures of the Bacterial Ribosome at 3.5 Å Resolution. *Science* **2005**, *310*, 827–834. [CrossRef] [PubMed]
17. Kabsch, W. XDS. *Acta Crystallogr. Sect. D Biol. Crystallogr.* **2010**, *66*, 125–132. [CrossRef] [PubMed]
18. McCoy, A.J.; Grosse-Kunstleve, R.W.; Adams, P.D.; Winn, M.D.; Storoni, L.C.; Read, R.J. Phaser crystallographic software. *J. Appl. Crystallogr.* **2007**, *40*, 658–674. [CrossRef] [PubMed]
19. Murshudov, G.N.; Skubak, P.; Lebedev, A.A.; Pannu, N.S.; Steiner, R.A.; Nicholls, R.A.; Winn, M.D.; Long, F.; Vagin, A.A. REFMAC5 for the refinement of macromolecular crystal structures. *Acta Crystallogr. Sect. D Biol. Crystallogr.* **2011**, *67*, 355–367. [CrossRef] [PubMed]
20. Emsley, P.; Lohkamp, B.; Scott, W.G.; Cowtan, K. Features and development of Coot. *Acta Crystallogr. Sect. D Biol. Crystallogr.* **2010**, *66*, 486–501. [CrossRef] [PubMed]
21. DeLano, W.L. The PyMOL Molecular Graphics System. Available online: http://www.pymol.org/ (accessed on 11 January 2016).